Stewart, B. W., G. E. Bebout, and M. Grove. 1992. Miocene magmatism in a transcurrent tectonic setting: isotopic data from Santa Catalina Island, California. Eos Transactions of the American Geophysical Union 73:338.

Thompson, R. N., M. A. Morrison, G. L. Hendry, and S. J. Parry. 1984. An assessment of the relative roles of a crust and mantle in magma genesis: an elemental approach. Philosophical Transactions of the Royal Society of London A310:549–590.

Turner, D. L. 1970. Potassium-argon dating of Pacific Coast Foraminiferal Stages. Geological Society of America Special Paper 124:91–129.

Vedder, J. G., and D. G. Howell. 1976. Neogene strata of the southern group of Channel Islands, California. In: Aspects of the Geologic History of the California Continental Borderland (edited by D. G. Howell), Pacific Section, American Association of Petroleum Geologists Miscellaneous Publication 24, pp. 80–106.

Vedder, J. G., D. G. Howell, and J. A. Forman. 1979. Miocene strata and their relation to other rocks, Santa Catalina Island, California. In: Cenozoic Paleogeography of the Western United States (edited by J. M. Armentrout, M. R. Cole, and H. TerBest, Jr.), Pacific Section, Society of Economic Paleontologists and Mineralogists, Pacific Coast Paleogeography Symposium 3:239–256.

Vedder, J. G., H. G. Greene, S. H. Clarke, and M. P. Kennedy. 1986. Geologic map of the mid-southern California continental margin. In: Geologic Map Series of the California Continental Margin (edited by H. G. Greene and M. Pp. Kennedy), California Division of Mines and Geology, Plate 2A, scale 1:250,000.

Weigand, P. W. 1994. Middle Miocene igneous rocks in the El Modeno, San Joaquin Hills, and Laguna Beach areas, southern California. In: Field Geology in Orange County, Southern California (edited by P. Hughes, R. P. Lozinsky, and G. R. Roquemore), Far Western Section National Association of Geology Teachers Guidebook, pp. 55–84.

Weigand, P. W., and K. L. Savage. 1993. Review of the Miocene volcanic rocks of the western Santa Monica Mountains, California. In: Miocene Sedimentary and Volcanic Environments, Santa Monica Mountains, California (edited by P. W. Weigand, A. E. Fritsche, and G. E. Davis), Society for Sedimentary Geology, Pacific Section, Book 72, pp. 93–112.

Wilson, M. 1989. Igneous Petrogenesis. Unwin and Hyman, London, 466 pp.

Wood, W. R. 1981. Geology, petrography and geochemistry of the Santa Catalina Island volcanic rocks, Black Jack Peak to Whitley's Peak area [M. S. Thesis]. California State University, Los Angeles, 146 pp.

Yeats, R. S. 1968. Rifting and rafting in the southern California borderland. In: Conference on Geologic Problems of the San Andreas Fault System (edited by W. R. Dickinson and A. Grantz), Stanford University Publications in Geological Sciences 11:307–322.

The Fourth California Islands Symposium: Update on the Status of Resources
Edited by W. L. Halvorson and G. J. Maender. 1994. Santa Barbara Museum of Natural History, Santa Barbara, CA.

Faulting and Uplift of the Northern Channel Islands, California

Christopher C. Sorlien

Institute for Crustal Studies, University of California, Santa Barbara, CA 93106
Tel. (805) 893-8231; Fax (805) 893-8649

Abstract. The northern Channel Islands are aligned E–W along the southern margin of the rotated western Transverse Ranges. Continuing post-Miocene clockwise rotation of the western Transverse Ranges is related to oblique left-reverse deformation of the northern Channel Islands. Strain partitioning is indicated by the presence of sub-horizontal striations on fault surfaces of both outcrop-scale and island-scale faults. Uplifted wavecut platforms are present in the footwalls (downthrown blocks) of the steeply-dipping mapped faults, and must be the result of thrust motion above sub-horizontal faults. On eastern Santa Cruz Island, as the upper crust moves southward relative to the deeper crust, new oblique-slip faults are progressively forming to the north.

The time that the islands have been emergent can be calculated from the elevation of the islands, the rock uplift rate, and the erosion rate. Because the wavecut rock platforms have yet to be dated, the uplift rate is not known. Well preserved wavecut platforms in volcanic rocks suggest that denudation of the highest peaks has been slow, and that uplift must have been at least a kilometer since important shortening initiated at the end of early Pliocene time. Large permanent islands have only been present for ~3 My, or ~2 My if shortening and uplift rates have increased with time.

Keywords: California; western Transverse Ranges; northern Channel Islands; rotation; uplift; faulting; striations; marine terraces; strain partitioning.

Introduction

The northern Channel Islands lie along the southern margin of the western Transverse Ranges, south of Santa Barbara Channel (Fig. 1). The Transverse Ranges are

Compiled from: Greene and Kennedy (1989); Jennings and Strand (1969); PG&E (1988); Junger and Wagner (1977); This Study

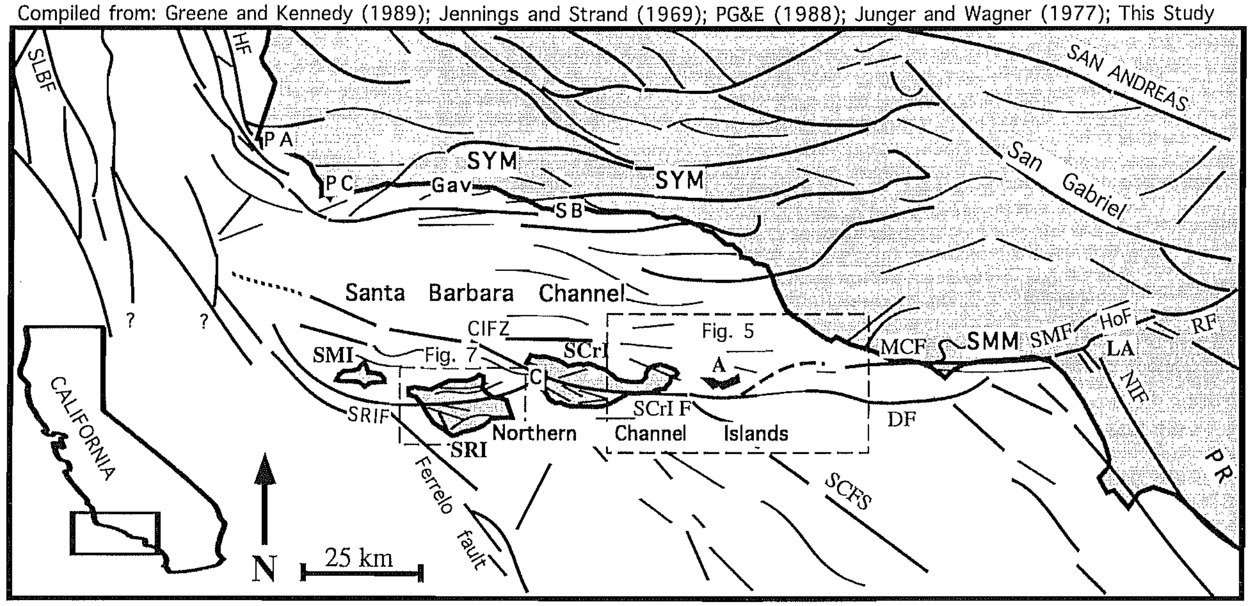

Figure 1. Faults and locations of the western Transverse Ranges. Geographic abbreviations include: **A** = Anacapa Island; **C** = Christi outcrop; **Gav** = Gaviota; **LA** = Los Angeles; **PA** = Point Arguello; **PC** = Point Conception; **PR** = Peninsular Ranges; **SB** = Santa Barbara; **SCrI** = Santa Cruz Island; **SMM** = Santa Monica Mountains; **SMI** = San Miguel Island; **SRI** = Santa Rosa Island; **SYM** = Santa Ynez Mountains; the western Transverse Ranges are the region of E-W faulting. Structural abbreviations include: **CIFZ** = Channel Islands fault zone of Ogle (1984); **DF** = Dume fault; **HF** = Hosgri fault; **HoF** = Hollywood fault; **MCF** = Malibu Coast fault; **NIF** = Newport-Inglewood fault; **RF** = Raymond fault; **SCFS** = San Clemente fault system (along the eastern escarpment of Santa Cruz-Catalina ridge); **SCrIF** = Santa Cruz Island fault; **SMF** = Santa Monica fault; **SRIF** = Santa Rosa Island fault; **SLBF** = Santa Lucia Bank fault.

unusual in California in that their topography, and the faults and folds affecting that topography, are oriented east–west. Paleomagnetic measurements indicate that the western Transverse Ranges have been clockwise rotated 90° or more in the last 17 My (Kamerling and Luyendyk 1979, 1985; Luyendyk et al. 1985). In new models, a thin sheet of upper-plate western Transverse Ranges crust rifted away from the Peninsular Ranges, and was transported above sub-horizontal detachment faults (Crouch and Suppe 1993). Santa Cruz and Santa Rosa islands are located along the trailing edge of this rotating sheet, and were originally located west of San Diego (see Abbott and Smith 1989; Kamerling and Luyendyk 1979). To the east, the Santa Monica Mountains are part of the same structural trend as the islands.

Paleomagnetic data support continuing clockwise rotation to present (Hornafius et al. 1986; Luyendyk 1991). New results from space-based geodetic techniques indicate that the western Transverse Ranges continue to rotate today, that a component of strike-slip motion on east–west faults is likely, and that NNE–SSW shortening between Santa Cruz Island and the Santa Ynez Mountains is more than 6 mm/yr (Hager et al. 1993; Larson and Webb 1992; Larsen et al. 1993; Jackson and Molnar 1990; Molnar 1992a). Folding of the sediments documents significant post-Miocene shortening of the islands, Santa Barbara Channel, and the mainland; this shortening becomes greater to the east (Namson and Davis 1992; Shaw and Suppe 1991, 1994; Sorlien 1994). This shortening reactivated Miocene faults, propagated into the offshore during Pliocene time, and drove continuing rotation.

There is currently a controversy regarding the importance of present-day strike-slip vs dip-slip motion in the western Transverse Ranges (Namson and Davis 1988; Davis et al. 1989; Shaw and Suppe 1991; Pinter and Sorlien 1991; Dolan and Sieh 1992). How is NNE–SSW shortening across the western Transverse Ranges accommodated in the northern Channel Islands region?

Faulting along the Trailing Edge of the Western Transverse Ranges

The Santa Cruz Island and Santa Rosa Island faults each run E–W down the axis of their namesake islands, and continue offshore. Both the north branch of the Santa Cruz Island fault and the eastern half of the Santa Rosa Island fault dip north with normal separation on Miocene and older rocks and generally reverse (north side up) separations on Pleistocene terrace deposits. Offshore to the west, a broad zone of WNW-striking faults was mapped on the northern Channel Islands ridge (Junger 1979). A major fault system, the "Channel Islands fault zone" (CIFZ) (Fig. 1), has been mapped north of Santa Cruz Island, but never described (Ogle 1984; Ogle et al. 1987).

These faults interconnect with the southern frontal faults of the western Transverse Ranges located farther east such as the Dume (DF), Malibu Coast (MCF), Santa Monica (SMF), Hollywood (HoF), and Raymond (RF) faults (Junger and Wagner 1977; Pinter and Sorlien 1991) (Fig. 1). Numerous regional studies suggest large (32–90 km), but conflicting estimates of Neogene sinistral slip, or late Neogene sinistral slip (15 km post 8 Ma, tens of kilometers post early Miocene) (Campbell and Yerkes 1976; Truex 1976; Dibblee 1982a; Wright 1991; Savage and Despard 1990). Restoring 50–75 km of left slip along the Channel Islands would align the Ferrelo fault system with similar E-dipping faults to the north such as the Santa Lucia Bank (SLBF) fault (Fig. 1).

Both the existence of significant Quaternary slip and the nature of any slip have been controversial on the Santa Monica-northern Channel Islands faults. Significant slip on the Santa Monica system is thought to have ended before late Pliocene time (Wright 1991; Davis et al. 1989). However, trenching has recently confirmed important late Quaternary lateral motion on the Malibu Coast, Santa Monica, Hollywood, and Raymond faults (Crook et al. 1987; Rzonca et al. 1991; Dolan and Sieh 1992; Dolan et al. 1993). Offset ravines indicate that the Santa Cruz Island fault has an important Quaternary sinistral component (Patterson 1979; Pinter and Sorlien 1991). Geologic relations that suggested that the Santa Cruz Island fault has not been Holocene active have been demonstrated to be incorrect (Pinter and Sorlien 1991; Sorlien and Pinter 1991; Sorlien 1992). Except for Dibblee (1982b), little has been published on late Quaternary activity of the Santa Rosa Island fault.

Santa Cruz Island Fault: Field Studies

The Santa Cruz Island fault is the most important fault exposed on the islands, with tens of kilometers of Neogene slip, and the clearest evidence for continuing late Quaternary motion. However, the western third and much of the central part of the Santa Cruz Island fault is atypical of the overall fault system in that the majority of late Quaternary activity is concentrated in a narrow zone along the north branch. Both the south and north branches of the Santa Cruz Island fault separate dissimilar Miocene and older rocks. The south branch shows much less systematic evidence for Quaternary activity than does the north branch (Patterson 1979).

On the eastern part of the island the fault branches and strands to the north of the main Neogene fault zone accommodate much of the late Quaternary activity. North of Valley Anchorage, a rock avalanche landslide crosses the zone of active faulting (Fig. 2). This landslide has been dated at 12,780 +/– 390 BP using charcoal from deep below the landslide surface in a ravine at location "a" on Figure 2. The landslide is composed of nearly 100% Monterey Formation, which originated in outcrops to the north of the main strand of the Santa Cruz Island

Geology after Weaver and Nolf (1969); Faults after Patterson (1979)

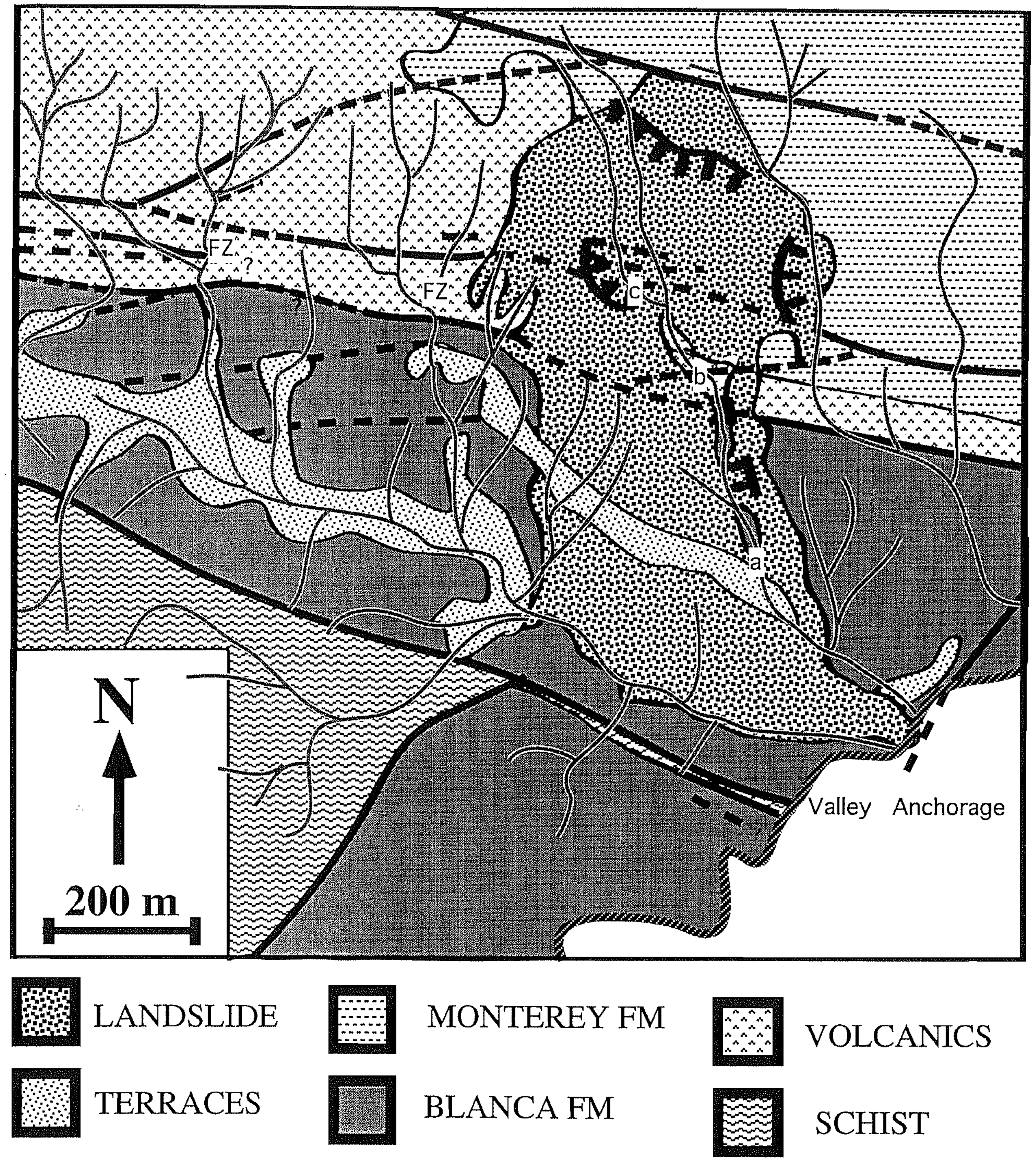

Figure 2. Map of landslide on Santa Cruz Island, with the northern branches of the Santa Cruz Island fault crossing the northern part of the landslide. Letters apply to locations mentioned in the text. The drainage pattern is in gray, and the faults are black.

fault. Shattered dolomite beds can be traced for tens of meters within blocks of Monterey Formation that rafted along the avalanche, but more commonly, the material is broken into chaotically oriented fist sized chunks.

I interpret the fault system to have moved since the landslide covered it. A ravine has eroded through the landslide into Miocene rocks along much of its length. At location "b" (Fig. 2), a fault zone is exposed in volcanic

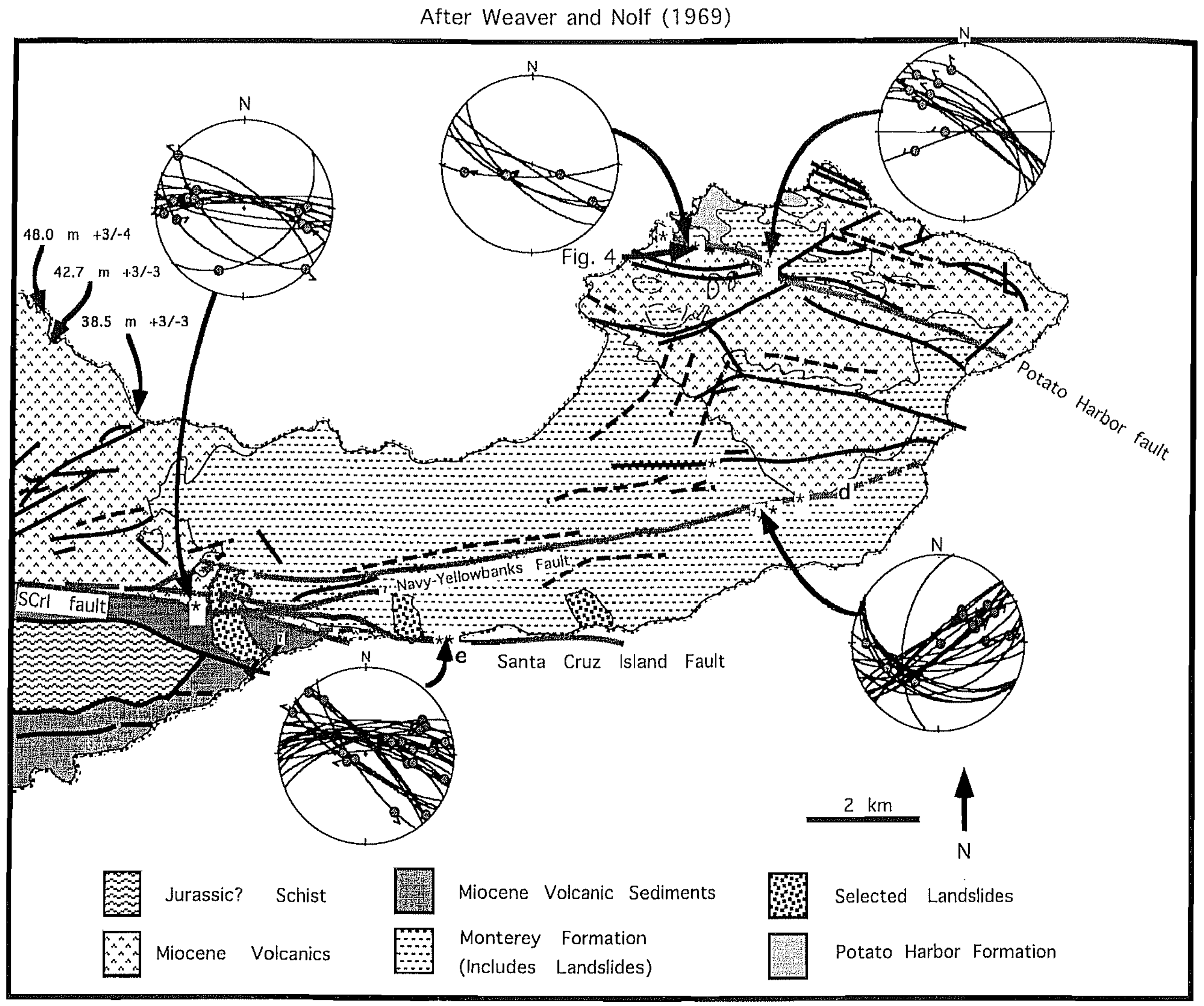

Figure 3. This fault map of the eastern half of Santa Cruz Island was modified from Weaver and Nolf (1969) and Patterson (1979). The letters apply to locations mentioned in the text. Fault measurements are shown on the lower hemisphere of an equal-area net; the curves are the planes, and the circles are the striations. Arrows pointing inward have a reverse component of slip, while those pointing outward have a normal component: sense was interpreted directly from the striations on only part of these measurements. Faults with evidence for late Quaternary activity are shown as gray. The elevations are shoreline angle measurements, with errors in meters, at Prisoners Harbor and Pelican Harbor.

rocks and is associated with a left deflection of the ravine. Fractures extend upwards into landslide material but do not provide conclusive proof of post-landslide activity. To the west of the landslide, the clearest left stream offsets are associated with a fault strand located to the north of the main Neogene fault. This strand projects across the landslide near location "c" (Fig. 2). At "c", the chaotically oriented landslide material is sheared in NE-striking zones a few to a few tens of centimeters thick. These zones are distinct from shearing expected during the landsliding process along the edge of the larger rafted blocks. Scaled fault experiments suggest that an E–W left-lateral strike slip fault will form ENE–WSW R (Riedel) shears in a weaker cover material (Wilcox et al. 1973). Therefore, discontinuous, ENE to NE-striking fault strands are expected in the landslide material if the underlying fault has been active. Left deflections of ravines cut into landslide material are present, but can not be clearly projected from one ravine to the next.

Several fault strands continue to the east of the landslide. The geometry of each strand, the thickness and composition of the fault zone, and the sharpness of related stream offsets all depend on the rock type, cumulative Neogene slip, and late Quaternary slip rates. A northern system (informally named Navy-Yellowbanks fault in Fig. 3), is associated with systematic left bends of canyons and sharp left offsets of smaller ravines, even though it has less than 100 m of vertical separation on beds of the mid-

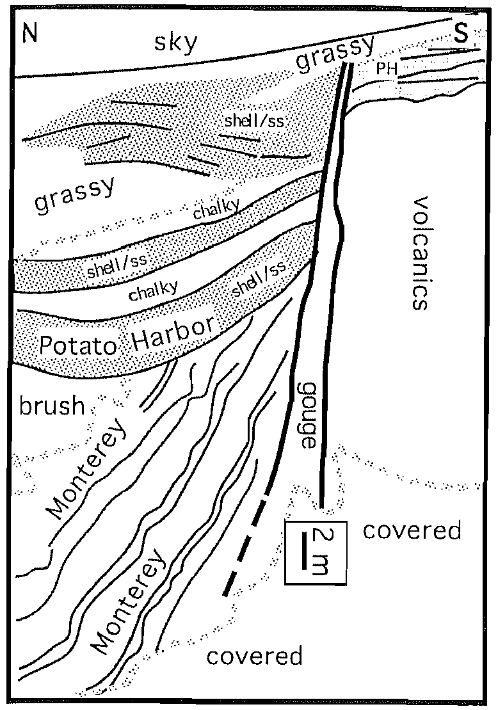

Figure 4. This is a tracing of a photograph, viewed to the east of the Potato Harbor fault, taken from the top of a ridge to the side of a steep, west-facing slope (see Fig. 3 for location). The 2-m scale is from a vertical person in the photograph. The steep fault (heavy black lines) separates the steeply N-dipping Monterey Formation (lower left) from the Santa Cruz island volcanics (right; massive, bedding not determined). Above an angular unconformity (center), the Pleistocene Potato Harbor Formation is faulted against the volcanics and more Potato Harbor Formation (PH, upper right). Within the Monterey Formation, thin dark lines are chert beds, and thin gray lines are bedding within a chalky unit. Dotted beds of the Potato Harbor Formation are gray, shell-rich sandstone; the upper portion is cross-bedded. Black curves within the Potato Harbor Formation represent bedding and cross bedding; some of the change in apparent dip is due to topography. The white interbeds are white in color, and the gray units at the upper right (PH) are white with some shell-rich gray inter-beds. Striations were measured along the edges of the gouge zone (Fig. 3).

Miocene Monterey Formation. Sub-vertical strands of this fault abruptly flatten down dip and along strike to parallel moderately dipping beds, as seen in excellent 3-dimensional canyon exposures. Striations on bedding parallel shear zones support a significant component of lateral slip on these surfaces. At location "d" (Fig. 3), a wide zone of deformed Monterey Formation contains numerous bedding-parallel slip surfaces. Farther north, a left-oblique (south side up) fault system is associated with very prominent scarps (informally named Potato Harbor fault in Fig. 3), and faults the Quaternary Potato Harbor Formation (Fig. 4; see Weaver and Meyer 1969; Weaver and Nolf 1969). This fault has about 100–150 m vertical separation on the base of the Monterey Formation, with smaller vertical separation across nearby sub-parallel faults.

The wide zone of distributed faulting that characterizes eastern Santa Cruz Island is also characteristic of the offshore region farther east. East of Anacapa Island, seismic reflection data image late Quaternary faults that are widely distributed across strike (Fig. 5). The Dume fault has a north-side up seafloor scarp and aligns with the Santa Cruz Island fault, but its shallow portion dies out within Quaternary deposits of the Hueneme fan. The Malibu Coast fault also deforms the seafloor, but is misaligned with the Santa Cruz Island fault across a 6-km left step (Fig. 5). Both the Channel Islands fault zone of Ogle et al. (1984) and faults exposed on eastern Santa Cruz Island align with the Malibu Coast fault. Additional lateral slip is likely transferred northwards from the Santa Cruz Island fault via NE-striking faults forming the southeastern margin of Anacapa ridge (Fig. 5). Displacement is transferred northwards across stepovers by through-going NE-striking faults strands both onshore and offshore (Figs. 3 and 5).

On eastern Santa Cruz Island and in the offshore region to the east of Anacapa Island, substantial Quaternary strain is accommodated by faults with small vertical separation of Miocene rocks. Both the northern margin of the Los Angeles basin, an area of poor outcrop and little public seismic reflection data, and the area east of Anacapa Island have a south-directed motion of the hanging-wall above gently N-dipping faults. It follows that many late Quaternary faults remain to be discovered to the north of the Santa Monica fault, especially in any step-over region.

Striation Measurements on Santa Cruz Island

I have measured the attitudes of striations on more than 500 surfaces on Santa Cruz and Santa Rosa islands. These measurements give the direction, and where determined, the sense of the last slip on each fault, but do not indicate when that slip occurred. Most striations were non-mineralized abrasion features. Measurements are divided into (1) those on faults with millimeters to a few meters of slip in the interior of kilometer-scale fault blocks; (2) those on or within a few tens of meters of mapped faults without clear evidence of late Quaternary slip, and (3) those on the last active surfaces of faults active during late Quaternary time. It is likely that most through-going fractures within a deforming zone would suffer some displacement, and that the observed abrasions are the result of the latest movement of the larger zone. Care was taken within the larger fault zones to measure only through-going surfaces.

Figure 6a is a rose diagram of measurements taken on the western half of Santa Cruz Island during 1988, excluding those from within the fault zones of larger mapped faults (Weaver and Nolf 1969). Within a limited

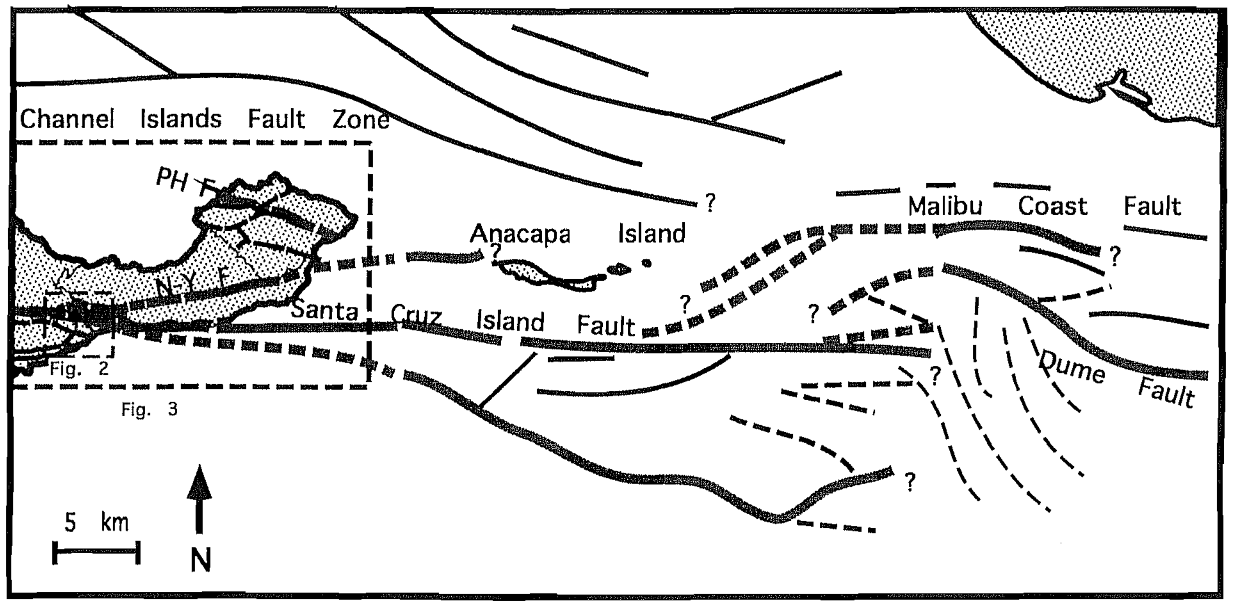

Figure 5. Fault pattern on eastern Santa Cruz Island and near-seafloor pattern beneath the Hueneme Fan; see Figure 1 for location. Heavy, grayed lines on this preliminary map indicate faults that cut Quaternary sediments onshore, deflect streams, deform the seafloor, or cut the youngest Quaternary offshore seismic sequence. Minor faults and fault-controlled channels are indicated by light dashed lines. South and west of Anacapa island, the interpretation is from Junger and Wagner (1977), while the interpretation north of Santa Cruz Island is from Ogle et al. (1987). East of Anacapa island, U.S. Geological Survey data set 19236 was used by both Burdick and Richmond (1982) and this study. The location of Figures 2 and 3 are shown by the dashed boxes.

area, all in-place faults with striated surfaces were measured. From the figure, it is clear that either dip-slip motion never affected the interior of kilometer-scale fault blocks, or older striations are not preserved and the youngest motion has been horizontal. Determination of the sense of slip was attempted for all measurements in Figure 6a. The preferred strike of these faults is north–northeast; these faults are mostly right-lateral.

Figure 6b is a bar graph of measurements within the deformed zone of mapped faults on Santa Cruz Island, and includes many measurements from the Alamos and Willows faults of southern Santa Cruz Island (see Weaver and Nolf 1969). The aim of these measurements was to determine the direction of slip of the mapped faults; therefore, fault surfaces that were sub-parallel to the mapped faults were preferentially measured. Slip is predominantly horizontal to oblique, with normal-dextral slip on the Alamos fault and mainly reverse-sinistral motion on the Willows fault to the east.

Measurements associated with late Quaternary active strands of the Santa Cruz Island fault have also been grouped (Fig. 6c). These measurements are predominantly sub-horizontal, with both normal and reverse oblique components. Several of the steeply pitching measurements were from through-going fractures that cut gouge at the Christi outcrop ("C" in Fig. 1) of the Santa Cruz Island fault. At this outcrop, radiocarbon dates from a buried organic layer below a sequence boundary and from a small charcoal grain above that boundary are > 36,300 and > 47,000, respectively, indicating an extremely slow rate of vertical separation (< 0.1 mm/yr). Evidence for compression and very slow rates of vertical separation contrasts with observations of the fault made farther east.

To the east, about 1 km east of where the main strand separating Blanca Formation from the Santa Cruz Island volcanics crosses the coastline, another important strand of the Santa Cruz Island fault system crosses the coast (location "e" on Fig. 3). Like at the Christi outcrop, obvious planar through-going fractures cut a 9-m thick zone of reconsolidated gouge; these fractures are located near the margins of the zone. The latest slip occurred on an anastomosing fault network a few centimeters thick located within a few centimeters of the northern edge of the zone. Well developed, deeply incised striations on hard clay gouge pitch east ~10 to ~30°, consistent with left-lateral motion with a small component of reverse slip. However, less than 1 m to the south, a slightly more mineralized fault surface has well developed striations that pitch east ~65°, or reverse with a left-lateral component. Creep is not likely, as randomly oriented elongate gypsum crystals overlie the striations. Although late Quaternary motion on the Santa Cruz Island fault was primarily strike-slip, these observations indicate that it is also capable of reverse movement.

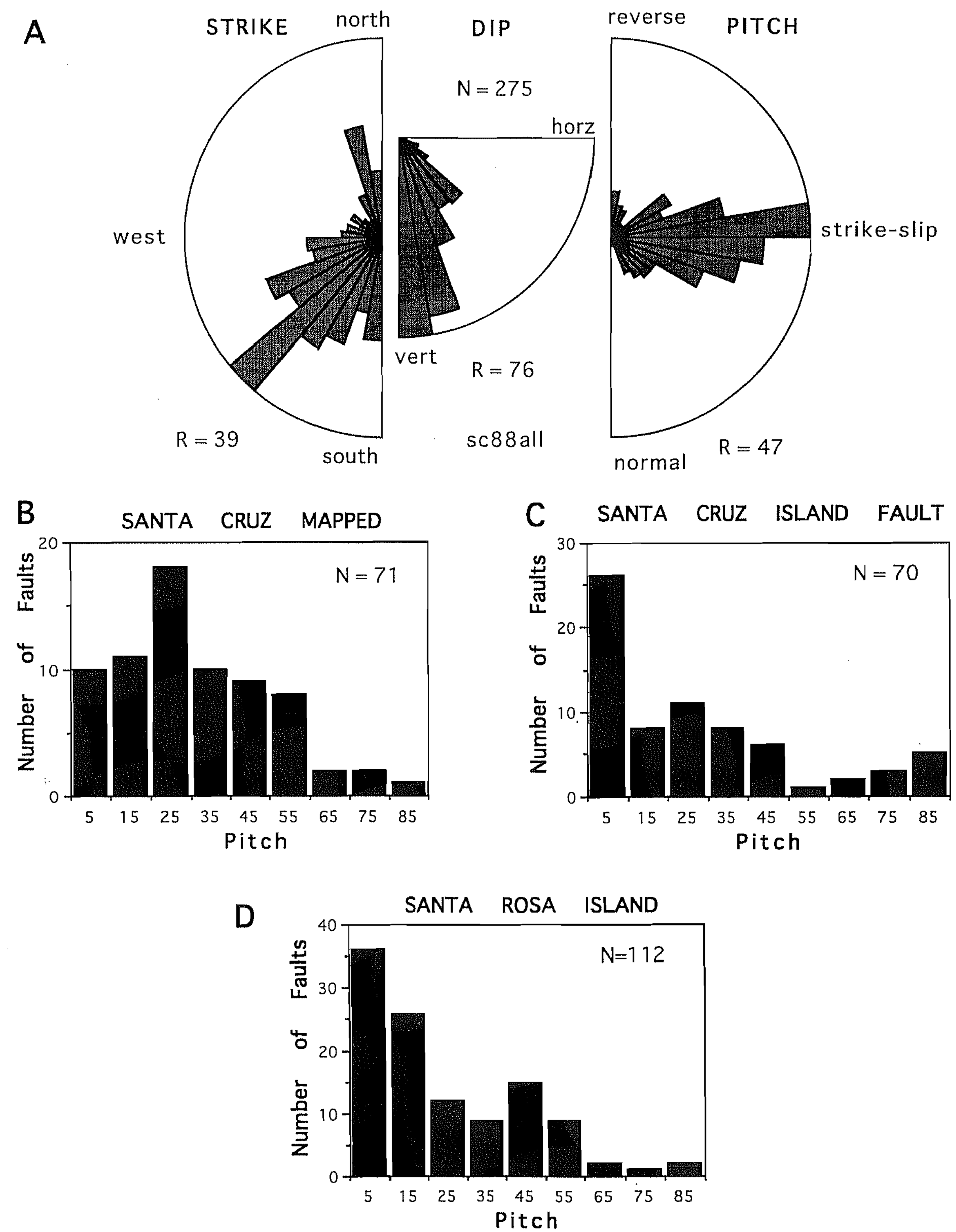

Figure 6. 6A. Rose diagrams indicate that slip on 275 minor (a few mm to a few cm of slip in most cases) faults on the western half Santa Cruz Island are primarily steeply dipping, and that the latest motion on fault surfaces is overwhelmingly horizontal. **6B.** 71 Striation measurements from surfaces within on mapped fault zones on Santa Cruz Island. Strike-slip is to the left, and dip-slip is to the right. **6C.** 70 striation measurements of faults dipping ≥ 45°, and striking from 75-135° that are associated with active strands of the Santa Cruz Island fault. **6D.** 112 striation measurements from mapped faults on northern Santa Rosa Island, limited to dip ≥ 45° and strike from 35–130°.

A few hundred meters west of this outcrop, the same fault strand deforms shales of the Monterey Formation. The character of the fault is entirely different, with a more ductile deformation across a zone tens of meters thick. A crude stretching lineation is present on subvertical layering (sheared bedding) within the zone; this lineation pitches gently east, consistent with the youngest striations on the more brittle outcrop.

Santa Rosa Island Fault

The Santa Rosa Island fault branches from the Santa Cruz Island fault near the west coast of Santa Cruz Island, with the Santa Cruz Island fault continuing westward in the offshore north of Santa Rosa Island (Fig. 1). The Santa Rosa Island fault places Miocene sediments to the north in contact with older Miocene sediments and volcanic rocks to the south across a thick crushed and sheared zone (few to more than 10 m thick). Weaver (1969) proposed 16 km of left-horizontal slip on the Santa Rosa Island fault since the deposition of early Miocene (?) volcanic sediments. This fault has down-to-the north separation on Miocene rocks, and dips north along its eastern portion. Although the Santa Rosa Island fault appears to be an important Neogene structure, minimal activity is likely during the last few tens of thousand years. This evidence includes the following:

1. Left deflections of major streams do not occur at the fault trace; instead deflections occur upstream of (south of) the fault. These deflection range from 250 to 1,400 m.
2. Smaller gullies are not systematically deflected at the fault.
3. There is only a small offset of the low wave-cut platform at the fault and a correspondingly larger, but still small, offset of a higher terrace.

The topographic map of Santa Rosa Island displays a prominent E–W-trending disruption of the contours that is related to the Santa Rosa Island fault. There are 8 major drainages that originate south of the Santa Rosa Island fault and flow northwards across it and then into Santa Barbara Channel or Santa Cruz Channel (Water Canyon) (Fig. 7a). All eight of these drainages flow westward parallel to and near the fault zone for distances ranging from 250 to 1,400 m (a tributary of Water Canyon flows eastward along the fault). Since all are deflected to the left near the fault, the first hypothesis is that these deflections are due to left-lateral motion on the fault. However, in several drainages (Arlington, Soledad west, Verde-west, and Water Canyon), the deflection today occurs south, or upstream of the fault by 50 to 100 m. Intact bedrock is continuously exposed through the left bend of the stream bed in Soledad west, and there is little evidence for faulting near the corresponding bend in the other drainages.

The deflection of the streams is too abrupt and systematic to be unrelated to the fault. A combination of a few tens of meters of sinistral slip, down-to-the-west tilting and topography at the fault could cause the large apparent offsets. Also, older inherited tectonic offsets may be preserved as the streams erode down and away from the fault.

Smaller ravines that cross the Santa Rosa Island fault should be offset at the fault if significant horizontal motion has occurred since ravine formation. Certain ravines have left deflections (e.g., location "f" and "g" on Fig. 7a) and many have no deflection. There is a strong contrast between these occasional deflections and the ubiquitous deflections of similar-sized gullies across the Santa Cruz Island fault. Examination of aerial photos confirms a lack of systematic gully deflection along the Santa Rosa Island fault.

Towards the west end of the island, an intermediate-sized ravine has a sharp 36-m left deflection at the fault ("g" on Fig. 7a). This ravine incises a marine terrace surface at 150 m elevation whose shoreline angle is about 25 m higher; the ravine is an unknown amount younger than the surface. An uplift rate of 0.5 mm/yr (see below) leads to the hypothesis that this 36-m offset occurred since < 330 Ka; a rate of > 0.11 mm/yr (see Hanson et al. 1990).

Another measure of the activity of the Santa Rosa Island fault is whether it offsets the top of the youngest wave cut platform, and whether it offsets overlying terrace deposits at the coast or stream terrace deposits inland. At the west end of the island, deposits of the higher marine terrace are clearly fractured by the fault at 130 m elevation. Between the west end and the sharp 36-m deflection, there is a prominent fault scarp or fault line scarp that offsets the terrace surface an estimated 10–20 m up to the south. At the east coast of Santa Rosa Island, the fault dips north and has a subtle minimum 1.5-m reverse separation of the low, wavecut platform (the dominant platform beneath the "Dume terrace" of Orr [1960a]). Stream erosion of the wavecut platform at the fault makes this a minimum figure; the elevation of the shoreline angle may change as much as 10 m at a distance from the fault (Fig. 7a).

The ENE-Striking Network of Fault Bands, Santa Rosa Island

Several faults have been mapped on Santa Rosa Island north of and striking sub-parallel to the Santa Rosa Island fault (Sonneman et al. 1969) (Fig. 7b). These faults are made up of dozens to hundreds of closely spaced individual sub-vertical fractures in zones 3–10 m thick. The fault bands, being slightly more resistant than the surrounding rock, form ridges a few tens of centimeters high that are quite visible across the higher marine terraces (location "h", Fig. 7a).

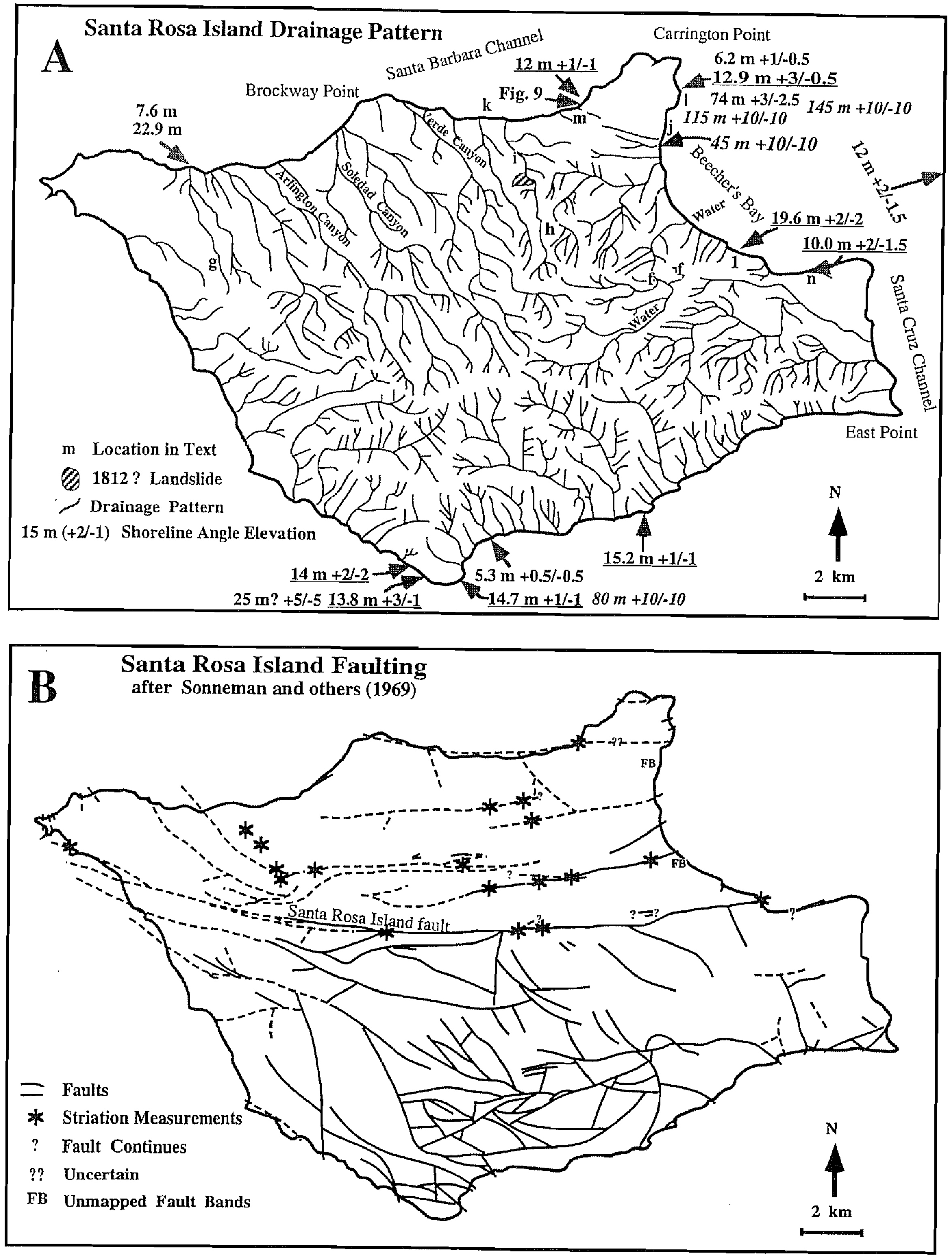

Figure 7. 7A. Drainage pattern of Santa Rosa Island; streams flow to the west along or just south of the Santa Rosa Island fault. Letters apply to locations mentioned in the text. Elevations are of shoreline angles; errors include estimating sea level, measurement errors, and uncertainty in location of the shoreline angle; those in italics were estimated from a contour map; the underlined measurements are interpreted to be the same age. **7B.** Faulting on Santa Rosa Island.

The resistance to erosion of these faults is related to the process of how faults form in sandstone. Most stations north of the Santa Rosa Island fault are located in a rhythmically bedded mid-Miocene sandstone. When sandstone is first faulted, the fault often becomes stronger than the surrounding rock, and the next fault forms a few centimeters away (Aydin 1978). The fault bands on Santa Rosa Island likely are the result of similar strain hardening, perhaps during single earthquakes.

The fault bands preserve different stages in the development of a gouge zone. The almost orderly arrangement of fault surfaces within the bands contrasts with the crushed to pulverized rock within the Santa Rosa Island fault zone; probably a much larger cumulative slip on that fault has caused the destruction of the original fault surfaces. Destruction of individual surfaces is under way at the thickest fault band (location "i" on Fig. 7a), where hundreds of closely spaced individual faults can barely still be distinguished.

Activity and Slip Direction of the Fault Bands, Santa Rosa Island

Mapped faults north of the Santa Rosa Island fault are most recently left-lateral strike-slip faults, and the Santa Rosa Island fault has had an important left-lateral component during the Quaternary. On Santa Rosa Island, striations were measured within the deforming zone of mapped and mappable (> ~10 m of vertical separation) faults. Again, horizontal slip predominates, with some of the oblique slip being normal separation (Fig. 6d). Normal separation fault surfaces tend to be mineralized, while strike-slip and reverse-left oblique faults show predominantly non-mineralized abraded striations. This is consistent with interpretation of offshore seismic reflection data that indicate that Miocene extension was followed by post-Miocene shortening (Sorlien et al. 1993; Sorlien 1994).

Three lines of evidence support left-horizontal slip on faults striking east to northeast:

1. Striations on surfaces within fault bands are sub-horizontal; measured surfaces include the largest fault within a zone. Where sense could be determined directly from the striations on E to NE-striking faults, the sense is left-lateral.
2. Layering in the rock does not match up consistently across the largest faults in canyons.
3. Scattered faults seen on sub-horizontal surfaces offset each other a few millimeters to a few tens of centimeters in a consistent manner (Locations "j" and "k", Fig. 7a). North-striking faults consistently offset E- and NE-striking faults to the right, while NE- to E-striking faults offset N-striking faults to the left. These conjugate fault systems clearly indicate NNE–SSW shortening, although the age of these faults is not known.

North of the Santa Rosa Island fault, I found no conclusive proof for activity on faults since the cutting of the low rock platform, and only subtle deflections of canyons cut into older marine terraces. Systematic stream deflections were not observed on aerial photographs. Along the east coast of Santa Rosa Island from Carrington Pt. to the Santa Rosa Island fault, there are only 2 locations where significant changes in height of the wave-cut platform are possible. Just north of the mouth of Water Canyon, a mapped fault band is covered by sand dunes where it intersects the coast, while at location "l", a ~1 m north-side up vertical separation of the rock platform could be either tectonic or due to differential erosion.

Stream and rock platform offsets support the idea that the Santa Cruz Island fault is many times more active than the Santa Rosa Island fault. Much of that motion must be accommodated on the westward continuation of the Santa Cruz Island fault, which passes offshore north of Santa Rosa Island.

Marine Terraces and Regional Uplift

Uplifted marine terraces are present along much of the California coast, as well as on all of the offshore Channel Islands. Santa Rosa Island and southwestern Santa Cruz Island are located on the downthrown block of the Santa Cruz Island fault, yet their landscapes are dominated by flights of uplifted marine terraces. Only a couple of meters of offset of the dominant low rock platform exists across the Santa Rosa Island fault, with lesser offsets or no offset across other faults. Therefore, the uplift of Santa Rosa and southwest Santa Cruz islands cannot be explained by slip on the mapped faults that cut the islands, and must be due to thrust or oblique motion on underlying gently dipping faults (Fig. 8).

A wavecut platform was traced semi-continuously along the eastern and northern coasts of the island to the northwest coast of Santa Rosa Island, where Orr (1960a) measured shoreline angle elevations of 25 and 75 ft (7.6 and 22.9 m). The shoreline angle (back edge or inner edge) is the break in slope between the paleo-sea cliff and the wavecut platform. It forms an originally horizontal datum that was cut slightly above the paleo-high tide level. A series of measurements of the shoreline angle suggest a tilt from an elevation near 20 m just north of the Santa Rosa Island fault, to 12 m at location "m", to 7.6 m on northwestern Santa Rosa Island (Fig. 9). Additional measurements are required near Brockway Point in order to confirm the down-to-the-west tilt, as more than one rock platform is exposed in the modern seacliff (Fig. 7a).

This shoreline angle is correlated across the Santa Rosa Island fault to a 10 m elevation at location "n", to a 15-m shoreline angle along the south-central coast, as well as to the lower (12 m) of a pair of rock platforms on the southwestern point of Santa Cruz Island (Fig. 7a). Measurements near East Point will be required to more confidently make these correlations, which are supported by the lack of a shoreline angle between 10 and 20 m at location "n" and by the down-to-the-south separation across the Santa Rosa Island fault. Remnant younger shoreline angles of 5.3 and 6.2 m were measured on south-central and northeast Santa Rosa Island, respectively, while the shoreline angle of a more prominent wavecut platform was nearly 75 m at both locations. Also at both locations, a possible rock platform intermediate between the 12 to 15 m and 75 m elevations is poorly preserved or does not exist, and is poorly exposed above location "j" (45 m +/– 10 m on Fig. 7a).

North-side-up reverse vertical separation of Quaternary material is present across the Santa Cruz Island fault (Pinter and Sorlien 1991). Near the midpoint of the north coast of Santa Cruz Island, the shoreline angle of the lowest wavecut rock platform is at ~40 m elevation (Fig. 3). The shoreline angle of a wide rock platform is between 100 and 120 m elevation on western Anacapa Island and northern Santa Cruz Island (estimated from topographic maps). The 40 m/110 m (+/–) pair on north-central Santa Cruz Island likely corresponds to the 13+ m/75 m pair on northeastern Santa Rosa Island.

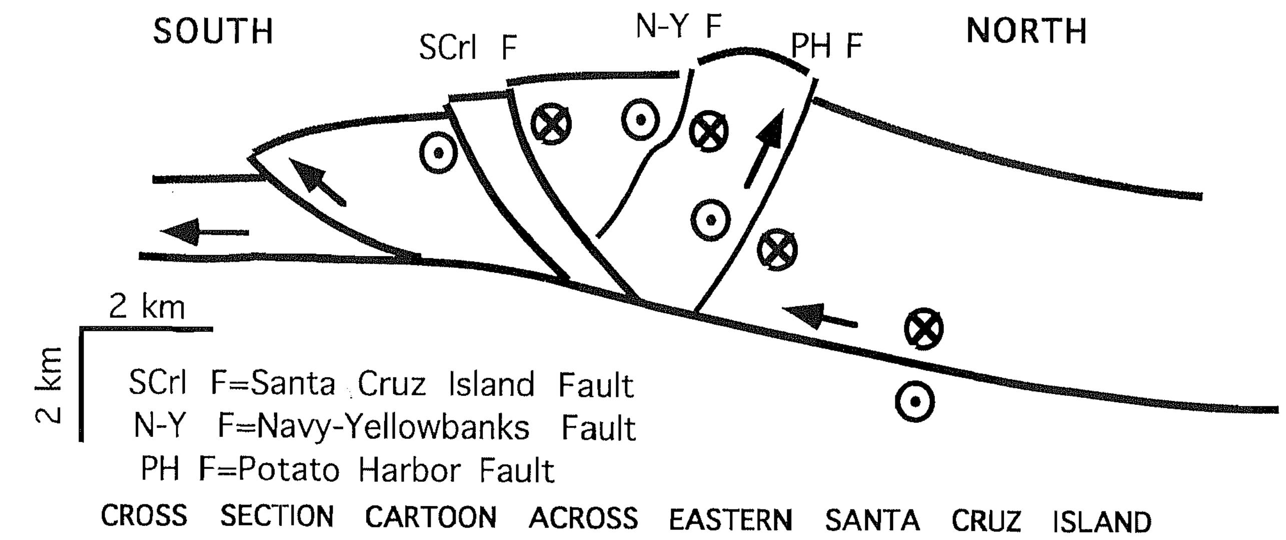

Figure 8. Cartoon cross section of eastern Santa Cruz Island.

Rapid or Slow Uplift?

Unfortunately, the wavecut rock platforms on the northern Channel Islands have not yet been dated, although on Santa Rosa Island I have recently collected marine shells and shell fragments from 2 rock platform levels and located shell material on a third level. However, the shell material collected from the 5.3 m to 6.2 m platform was too altered or replaced for a radiocarbon date to be meaningful; therefore, the samples were not dated (Darden Hood 1993, pers. comm.). Therefore, a series of logical arguments must suffice to support uplift rates of about 1 mm/yr north of the Santa Cruz Island fault, and about 0.5 mm/yr south of that fault. A radiocarbon date of 29,650 +/– 2500 BP (not corrected, from Orr 1960b, 1968) from half way up alluvial deposits on northwestern Santa Rosa Island is consistent with correlation of the 7.6-m wavecut platform to the eustatic sea level high stands at about 40,000 or 60,000 yr BP (–40 m and –25 m below present levels, respectively; Hanson et al. 1990). Because shell can form an open system with respect to uranium, I dismiss uranium-radium dates on shell material of > 135,000 and > 200,000 yr above the 7.6-m platform (Orr 1968; Muhs et al. 1992).

The remnant 5.3- to 6.2-m rock platform is very important to any attempt at matching elevations of shoreline angles to eustatic sea level curves (e.g., Lajoie 1986). Because uplift rates may vary with time and location, I will use shoreline angle elevations from 1 location: northeastern Santa Rosa Island (Fig. 7a). The eustatic sea level compilation of Hanson et al. (1990) includes the following pairs: 6 ka = 0 m; 40 ka = –40 m; 60 ka = –25 m; 80 ka = –5 m; 105 ka = –2 m, 125 ka = +6 m; and 210 ka = –3 m. Shoreline angle elevations include 6 m, 13+ m, 45 +/– m, 75 m, 115 +/– m, and 145 +/– m. The modern shoreline angle is between 2 and 3 m above mean seal level (MSL) (Rockwell et al. 1992a), so uplift rates are adjusted for 2 m lower elevations. While I would prefer to correlate the 6- to 13-m shoreline angle pair to the 40 and 60 ka highstands, matching the 6 m elevation to either 40, 60, or 80 ka and the 13+-m shoreline angle to the next older highstand requires tectonic subsidence. If the 6 m elevation corresponds to 6 ka, then the higher ele-

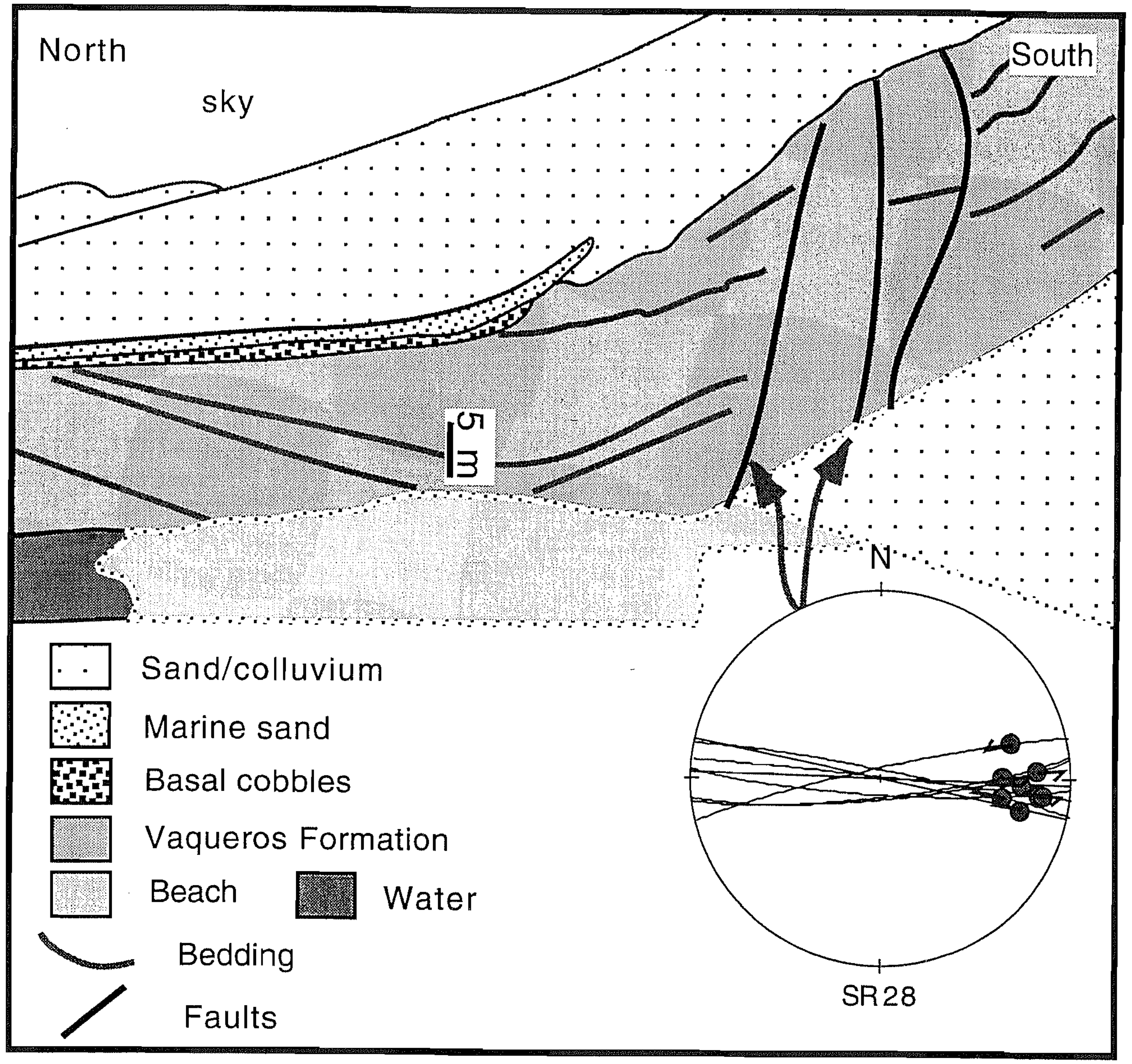

Figure 9. This is a tracing of a photograph, viewed to the east, of the shoreline angle of the low wavecut platform, with the Carrington fault to the right (south; sub-vertical black lines). Above a wavecut platform cut into late Oligocene and/or early Miocene Vaqueros Formation (sandstone with a few conglomerate layers), lies a basal cobble layer, a marine sand layer, and then colluvium. The vertical 5 m scale is at the base of a vertical cliff. The change in apparent dip within the Vaqueros Formation near the scale is due to change in orientation of the outcrop; the change in dip of the marine sand and basal cobbles is largely real. The equal area net shows striation measurements taken at this location; the left-reverse sense was determined from regional considerations and was not determined directly from the striations. See Figure 3 for description of the net, and Figure 7 for the location.

vations can be matched to the eustatic curve with a smoothly increasing with time uplift rate. Evidence for regression in the last few thousand years supports this correlation (Pinter and Sorlien 1991; Orr 1956).

Uplift rates adjusted for 2 m difference between MSL and shoreline angle for the following time intervals include: 6 m = 0–6 ka = 0.67 mm/yr; 40 ka not preserved; 13+ m = 60 ka = 0.59 mm/yr (6–60 ka); 45 m = 80 ka = 0.6 mm/yr (60–80 ka); 105 ka not preserved or compound with 125 ka; 75 m = 125 ka = 0.42 mm/yr (80–125 ka); 115 m = 210 ka = 0.58 mm/yr (125–210 ka). Errors in both eustatic level and the 45 and 115 m elevations might allow a smoother uplift rate. An uplift rate of ~0.5 mm/yr is only slightly higher than that determined by Rockwell et al. (1992b) at Gaviota (Fig. 1).

Interpretation of seismic reflection data in western Santa Barbara Channel indicate that shortening and uplift of the northern Channel Islands did not commence until early Pliocene time, and that rapid shortening is post-early Pliocene (Sorlien, 1994). Minor shortening in Santa Barbara Channel may have occurred near the end of Miocene time, but rapid shortening initiated near the end of early Pliocene time (Edwards and Heck 1994; J. Galloway, national assessment of undiscovered resources, Pacific offshore region, Santa Barbara Channel, 12 January 1994 presentation, Camarillo). The average rock uplift rate since shortening commenced is dependent on the water depth before uplift commenced and how much rock has been eroded from the highest peaks. Because wavecut rock platforms are present near the highest point of Santa Cruz Island (Rand 1933), it is likely that denudation in the volcanic rocks has not been important, and the islands have only been present slightly longer than their present elevation divided by the uplift rate. For example, a minimum 1 km of uplift since rapid shortening initiated at the end of early Pliocene time gives a minimum average uplift rate of 0.3 mm/yr; greater early Pliocene water depth and increase in shortening with time are likely. Because post-middle Miocene sediments are eroded away on the islands, the initial water depth is not known. However, foraminifera from wells north of Santa Rosa Island suggest early Pliocene mid to lower bathyal depths (public domain file for expired leases P-351 and P-358).

Uplift of a wide area of the northern Channel Islands at inferred rates between 0.5 and 1 mm/yr is consistent with the current 6 mm/yr of shortening across the channel (Larson and Webb 1992, Larsen et al. 1993). Part of this cross-channel shortening is accommodated along the northern shelf break of both Santa Rosa and San Miguel islands, where a fault on trend with the Channel Islands fault zone of Ogle (1984) dips south, and the corresponding fold verges to the north.

An alternate interpretation has been suggested. The 5.3- to 15-m rock platform pair on southern Santa Rosa Island may instead correspond to the 5a-5e highstands (80 ka and 125 ka) (T. Rockwell 1994, pers. comm.; G. Kennedy 1994, pers. comm.). This would require a much slower uplift rate than I have proposed. If this is the case, then it is likely that uplift was more rapid before late Quaternary time. If the islands are uplifting in response to shortening, and rapid shortening did not commence until the end of early Pliocene time, then large permanent islands were not present until that time, no matter what the rate is at present.

Fault Activity/Strain Partitioning

Surface uplift of northeastern Santa Cruz Island of about 1 mm/yr makes it unlikely that the faulted beach and non-marine shell deposits of the Potato Harbor Formation are early Pleistocene (see Weaver and Meyer 1969). Assuming a constant uplift rate, these deposits, located between 100 and 200 m elevation, must be late Pleistocene. The Potato Harbor Formation is cut by several faults on northeastern Santa Cruz Island, and their activity can be determined once the abundant shell material in the Potato Harbor Formation is dated.

In a region of oblique shortening, strain often partitions between co-existing thrust and strike-slip faults (Mount and Suppe 1987, 1992; Lettis and Hanson 1991; Molnar 1992b). Figure 8 shows a geometry where, with depth, the steeply dipping strike-slip and oblique-slip faults may flatten to merge with the gently dipping faults (see Shaw and Suppe 1994). In this case, oblique-slip on the decollement(s) is required beneath Santa Barbara Channel. The south-directed thrusting is related to the northwards migration of steeply-dipping hanging-wall faults discussed above. Alternatively, a strike-slip fault may be present in the footwall (below the thrust). As the hanging wall moves to the south relative to the footwall, hanging-wall strike-slip faults will progressively appear to the north; oblique slip is not required on the sub-horizontal fault beneath Santa Barbara Channel.

Conclusions

The axial faults that bisect Santa Cruz and Santa Rosa islands are part of a Holocene-active 200-km-long system that extends from Pasadena to west of San Miguel Island. Strike-slip motion on both major and minor faults predominates. The Santa Cruz Island fault appears to be much more active than the Santa Rosa Island fault. Therefore, activity probably continues on the offshore Santa Cruz Island fault north of Santa Rosa Island. Regional considerations and correlation of shoreline angles to eustatic curves support a late Quaternary rock uplift rate of about 0.5 mm/yr south of the Santa Cruz Island fault and 1 mm/yr north of it; this uplift rate requires that faults cutting the nearshore deposits of the Potato Harbor Formation be late Quaternary active. Because the islands are compressional fold structures, they were probably submerged until rapid shortening initiated in mid-Pliocene or later time. The left-horizontal motion on the mapped surface faults and the shortening across the islands, Santa Barbara Channel, and the mountains to the north are all part of the continuing clockwise rotation of thin sheets of crust.

Acknowledgements. This project would not have been possible without the facilities and transportation provided by the U.S. Navy, the Santa Cruz Island Reserve of the University of California, and the National Park Service. I would like to thank Shirley Clarke and Lyndal Laughrin of the University of California, and Kate Faulkner, Andrew Ovenden, Kevin Patterson, and Allen Fieldson of the National Park Service for their assistance. Scott Cranswick and Jim Galloway of the Minerals Management Service provided access to public data, as well as geologic input. The regional tectonic concepts benefited from discussions with Bruce Luyendyk and Craig Nicholson. Geological observations and discussions in the field of Joe Gasperi, Robin Weeks, Alec Tsongas, Freedom Johnson, Deborah Underwood, Jeff Myers, and Marc Kamerling are much appreciated. Discussions and observations with Nick Pinter improved my understanding of geomorphic features, and his writing of our geology paper provided a much-needed boost and focus to my work. A grant from the University of California, Santa Barbara Department of Geological Sciences covered a portion of my field expenses. The Institute for Crustal Studies contribution number was 0173-42TC.

Literature Cited

Abbott, P. L., and T. E. Smith. 1989. Sonora, Mexico, source of the Eocene Poway conglomerate of southern California. Geology 17:329–332.

Aydin, A. 1978. Small faults formed as deformation bands in sandstone. Pure and Applied Geophysics 116:914–930.

Burdick, D. J., and W. C. Richmond. 1982. A summary of geologic hazards for proposed OCS oil and gas lease sale 68, Southern California. Mineral Management Service and U.S. Geological Survey Open-File Report 82-33.

Campbell, R. H., and R. F. Yerkes. 1976. Cenozoic evolution of the Los Angeles basin area—relationship to plate tectonics. In: Aspects of the Geological History of the California Borderland: Pacific Section (edited by D. G. Howell), American Association of Petroleum Geologists, Miscellaneous Publication 24, pp. 541–558.

Crook, R., Jr., C. R. Allen, B. Kamb, C. M. Payne, and R. J. Proctor. 1987. Quaternary geology and seismic hazard of the Sierra Madre and associated faults, western San Gabriel Mountains. In: Recent Reverse Faulting in the Western Transverse Ranges, California (edited by D. M. Morton and R. F. Yerkes), U.S. Geological Survey Professional Paper 1339, pp. 27–64.

Crouch, J. K., and J. Suppe. 1993. Late Cenozoic tectonic evolution of the Los Angeles Basin and inner California Borderland: a model for core complex-like crustal extension. Geological Society of America Bulletin 105(11):1415–1434.

Davis, T. L., J. Namson, and R. F. Yerkes. 1989. A cross section of the Los Angeles area: seismically active fold and thrust belt, the 1987 Whittier Narrows earthquake, and earthquake hazard. Journal of Geophysical Research 94(B7):9644–9664.

Dibblee, T. W., Jr. 1982a. Geology of the Santa Monica Mountains and Simi Hills, southern California. In: Geology and Mineral Wealth of the California Transverse Ranges (edited by D. L. Fife and J. A. Minch), Mason Hill Volume, South Coast Geological Society, Santa Ana, California, pp. 94–130.

Dibblee, T. W., Jr. 1982b. Geology of the Channel Islands, southern California. In: Geology and Mineral Wealth of the California Transverse Ranges (edited by D. L. Fife and J. A. Minch), Mason Hill Volume, South Coast Geological Society, Santa Ana, California, pp. 27–39.

Dolan, J. F., and Sieh, K. E. 1992. Paleoseismology and geomorphology of the northern Los Angeles Basin: evidence for Holocene activity on the Santa Monica fault and identification of new strike-slip faults through downtown Los Angeles, Supplement to EOS. Transactions American Geophysical Union 73(43):589.

Dolan, J. F., K. E. Sieh, P. Guptill, G. Miller, T. Rockwell, and T. Smirnoff. 1993. Structural geology, fault kinematics, and preliminary paleoseismologic results from the Hollywood fault: new data from continuously cored borings and geotechnical trenches, Hollywood, California, Supplement to EOS. Transactions American Geophysical Union 74(43):427.

Edwards, E. B., and R. G. Heck. 1994. Structural model for Gato Canyon field, Santa Barbara Channel, California. Abstract, 69th Pacific Section AAPG, SEG, SEPM, AEG Meeting, Ventura, April 1994.

Greene, H. G., and Kennedy, M. P. (editors). 1989. Geology of the south-central California continental margin, California Continental Margin Geologic Map series, Area 4 of 7. Division of Mines and Geology.

Hager, B. H., A. Donnellan, and R. W. King. 1993. Space geodetic observation of block rotation and rapid convergence in the Ventura basin region, California. Geological Society of America, Abstracts with Programs 25(6):A-243.

Hanson, K. L., J. R. Wesling, W. R. Lettis, K. Kelson, and L. Mezger. 1990. Correlation, ages, and uplift rates of Quaternary marine terraces: south-central coastal california. Friends of the Pleistocene Pacific Cell, 1990 Fall Field trip, Field Trip Guidebook, Neotectonics of South-Central Coastal California, pp. 139–190.

Hornafius, J. S., B. P. Luyendyk, R. R. Terres, and M. J. Kamerling. 1986. Timing and extent of Neogene rotation in the western Transverse Ranges, California. Geological Society of America Bulletin 97:1476–1487.

Jackson, J., and P. Molnar. 1990. Active faulting and block rotations in the western Transverse Ranges, California. Journal of Geophysical Research 95:22073–22087.

Jennings, C. W., and R. G. Strand. 1969. Geologic map of California, Los Angeles sheet. California Division of Mines and Geology, Sacramento.

Junger, A. 1979. Northern Channel Islands Platform, California Continental Borderland. U.S. Geological Survey Map and Report MF991.

Junger, A., and H. C. Wagner. 1977. Geology of the Santa Monica and San Pedro Basins, California Continental Borderland. U.S. Geological Survey Map MF-820.

Kamerling, M. J., and B. P. Luyendyk. 1979. Tectonic rotations of the Santa Monica Mountains region, western Transverse Ranges, California, suggested by paleomagnetic vectors. Geological Society of America Bulletin, Part 1, 90:331–337.

Kamerling, M., and B. P. Luyendyk. 1985. Paleomagnetism and Neogene tectonics of the northern Channel Islands, California. Journal of Geophysical Research 90(B14):12485–12502.

Lajoie, K. R. 1986. Coastal tectonics. In: Active Tectonics (edited by R. E. Wallace), National Academy Press, Washington, D.C., pp. 95–124.

Larson, K. M., and F. H. Webb. 1992. Deformation in the Santa Barbara Channel from GPS measurements 1987–1991. Geophysical Research Letters 19(14):1491–1494.

Larsen, S. C., D. C. Agnew, and B. H. Hager. 1993. Strain accumulation in the Santa Barbara Channel: 1970–1988. Journal of Geophysical Research 98(B2):2119–2133.

Lettis, W. R., and K. L. Hanson. 1991. Crustal strain partitioning: implications for seismic-hazard assessment in western California. Geology 19:559–562.

Luyendyk, B. P. 1991. A model for Neogene crustal rotations, transtension, and transpression in southern California. Geological Society of America Bulletin 103:1528–1536.

Luyendyk, B. P., M. J. Kamerling, R. R. Terres, and J. S. Hornafius. 1985. Simple shear of southern California during Neogene time suggested by paleomagnetic declinations. Journal of Geophysical Research 90(B14):12454–12466.

Molnar, P. 1992a. Final report to the Southern California Earthquake Center for work performed during the period from September through December 1991, unpublished. 126 pp.

Molnar, P. 1992b. Brace-Goetze strength profiles, the partitioning of strike-slip and thrust faulting at zones of oblique convergence, and the stress-heat flow paradox of the San Andreas Fault. In: Fault Mechanics and Transport Properties of Rocks, Academic Press Ltd., pp. 435–459.

Mount, V. S., and J. Suppe. 1987. State of stress near the San Andreas fault: implications for wrench tectonics. Geology 15:1143–1146.

Mount, V. S., and J. Suppe. 1992. Present-day stress orientations adjacent to active strike-slip faults: California and Sumatra. Journal of Geophysical Research 97(B8):11995–12013.

Muys, D. R., G. H. Miller, J. F. Whelan, and G. L. Kennedy. 1992. Aminostratigraphy and oxygen isotope stratigraphy of marine-terrace deposits, Palos Verdes Hills and San Pedro areas, Los Angeles County, California. Marine and Lacustrine Systems, SEPM Special Publication no. 48, pp. 363–376.

Namson, J., and T. Davis. 1988. Structural transect of the western Transverse Ranges, California: implications for lithospheric kinematics and seismic risk evaluation. Geology 16:675–679.

Namson, J., and T. Davis. 1992. Late Cenozoic thrust ramps of southern California. Final Report for 1991 Contract, Southern California Earthquake Center.

Ogle, B. A. 1984. Significant new developments in the Santa Maria/Santa Barbara offshore California—the geology and economic potential. In: Proceedings of the Southwestern Legal Foundation, Exploration and Economics of the Petroleum Industry (edited by J. R. Moss), Matthew Bender and Company, Inc., New York, 22:23–81.

Ogle, B. A., W. S. Wallis, R. G. Heck, E. B. Edwards. 1987. Petroleum geology of the Monterey Formation in the offshore Santa Maria/Santa Barbara areas. In: Cenozoic Basin Development of Coastal California (edited by R. V. Ingersoll and W. G. Ernst), Ruby Colloquium, VI, University of California, Los Angeles, Prentice-Hall, pp. 382–406.

Orr, P. C. 1956. Radiocarbon dates from Santa Rosa Island, I. Santa Barbara Museum of Natural History, Bulletin no. 2, Santa Barbara, California.

Orr, P. C. 1960a. Late Pleistocene marine terraces on Santa Rosa Island, California. Geological Society of America Bulletin 71:1113–1120.

Orr, P. C. 1960b. Radiocarbon dates from Santa Rosa Island, II. Santa Barbara Museum of Natural History, Bulletin no. 3, Santa Barbara, California.

Orr, P. C. 1968. Prehistory of Santa Rosa Island. Santa Barbara Museum of Natural History, Santa Barbara, California. 253 pp.

Patterson, R. H. 1979. Tectonic geomorphology and neotectonics of the Santa Cruz Island Fault, Santa Barbara County, California. Masters thesis, University of California, Santa Barbara, Geology department. 140 pp.

Pinter, N., and C. C. Sorlien. 1991. Evidence for latest Pleistocene to Holocene movement on the Santa Cruz Island fault, California. Geology 19:909–912.
Pacific Gas and Electric Company. 1988. Final report of the Diablo Canyon long term seismic program. Pacific Gas and Electric Company, Docket nos. 50–275 and 50–323.
Rand, W. W. 1933. The geology of Santa Cruz Island, California. PhD thesis, University of California, Berkeley.
Rockwell, T. K., D. R. Muhs, and G. L. Kennedy. 1992a. Late Quaternary paleo-sea level estimates for the west coast of North America based on coral-dated marine terraces. International Geological Correlation Programme 274, International Symposium on Diversity in Coastal Evolution in the Quaternary, Programme and Abstracts, Annual Meeting, Wellington, New Zealand, p. 47.
Rockwell, T. K., J. Nolan, D. L. Johnson, and R. H. Patterson. 1992b. Ages and deformation of marine terraces between Point Conception and Gaviota, western Transverse Ranges, California. Marine and Lacustrine Systems, SEPM Special Publication no. 48, pp. 333–341.
Rzonca, G. F., H. A. Spellman, E. F. Fall, and R. J. Shlemon. 1991. Holocene displacement of the Malibu Coast Fault Zone, Winter Mesa, California: engineering geologic implications. Bulletin of the Association of Engineering Geologists 28(2):147–158.
Savage, K. L., and S. L. Despard. 1990. The Miocene Blanca Formation and Beecher's Bay member of the Monterey Formation, Santa Cruz Island, California: confirmation of stratigraphic correlation and petrogenesis of the volcanic clasts. Senior Thesis, Department of Geological Sciences, California State University, Northridge. 48 pp.
Shaw, J., and J. Suppe. 1991. Slip rates on active blind thrust faults in the Santa Barbara Channel, western Transverse Ranges fold and thrust belt, Supplement to EOS transactions. American Geophysical Union, 29 April 1991, 72(44):443.
Shaw, J. H., and J. Suppe. 1994. Active faulting and growth folding in the eastern Santa Barbara Channel, California. Geological Society of America Bulletin, in press.
Sonneman, H., D. W. Weaver, and D. Doerner, F. Avila, and other, anonymous authors. 1969. Geology of Santa Rosa Island. In: Geology of the Northern Channel Islands: AAPG and SEPM Pacific Section (edited by D. W. Weaver, D. P. Doerner and B. Nolf, Special Publication, map.
Sorlien, C. C. 1992. Structural style and strain partitioning in the northern Channel Islands, California, Supplement to EOS. Transactions American Geophysical Union 73(43):589.
Sorlien, C. C. 1994. Structure and evolution of the southern offshore Santa Maria Basin and western Santa Barbara Channel, California. PhD thesis, University of California, Santa Barbara.
Sorlien, C. C., C. Nicholson, B. P. Luyendyk, and M R. Legg. 1993. Miocene collapse of the California continental margin. Geological Society of America, Abstracts with Programs 25(6):A-311.
Sorlien, C., and N. Pinter. 1991. The northern Channel Islands fault system, California. Geological Society of America, Abstracts with Programs 23(5):A197.
Truex, J. N. 1976. Santa Monica and Santa Ana Mountains-Relation to Oligocene Santa Barbara Basin. American Association of Petroleum Geologists Bulletin 60(1):65–86.
Weaver, D. W. 1969. Paleogeographic implications and geologic history. In: Geology of the Northern Channel Islands: AAPG and SEPM Pacific Section (edited by D. W. Weaver, D. P. Doerner, and B. Nolf, Special Publication, pp.115–124.
Weaver, D. W, and G. L. Meyer. 1969. Stratigraphy of northeastern Santa Cruz Island. In: Geology of the Northern Channel Islands: AAPG and SEPM Pacific Section (edited by D. W. Weaver, D. P. Doerner, and B. Nolf), Special Publication, pp. 95–104.
Weaver, D. W., and B. Nolf. 1969. Geology of Santa Cruz Island. In: Geology of the Northern Channel Islands: AAPG and SEPM Pacific Section (D. W. Weaver, D. P. Doerner, and B. Nolf), Special Publication, map.
Wilcox, R. E., T. P. Harding, and D. R. Seeley. 1973. Basic wrench tectonics. American Association of Petroleum Geologists Bulletin 57(1):74–96.
Wright, T. L. 1991. Structural geology and tectonic evolution in the Los Angeles Basin, California. In: Active Margin Basins (edited by K. T. Biddle), AAPG Memoir 52, American Association of Petroleum Geologists, Tulsa, Oklahoma, pp.35–135.

The Fourth California Islands Symposium: Update on the Status of Resources
Edited by W. L. Halvorson and G. J. Maender. 1994. Santa Barbara Museum of Natural History, Santa Barbara, CA.

Lobo Canyon Landslide: Santa Rosa Island, California

John J. Wooley

Consulting Geologist, 1021 Via Cielito, Ventura, CA 93003
Tel. (805) 653-5633; Fax (805) 653-6153

Abstract. The Lobo Canyon Landslide, located in Lobo Canyon on the northeast coast of Santa Rosa Island, California, is a complex block slide. Its features include a series of linear pull-apart cracks or rifts defining the slide's headward area, and a zone of fractured bedrock and rockfalls, making up the zone of accumulation. The slide body has remained largely intact.

The southern boundary of the slide is determined by the location of a small fault: northern and eastern edges by northeast dipping bedding planes exposed in canyon walls. This feature has been discussed as the fault that generated a M = 7.0–7.5 earthquake on 21 December 1812. While it is clearly a landslide, it probably was initiated by an event of this magnitude and could have occurred during the 1812 quake.

Keywords: Santa Rosa Island; California Channel Islands; block slide; landslides caused by earthquakes; 21 December 1812 earthquake (Santa Barbara).

Introduction

The Lobo Canyon Landslide is a block-glide type slide occurring in Lobo Canyon (Cañada Lobos), Santa Rosa Island, California.

Santa Rosa Island (Fig. 1), 1 of the 8 islands offshore Southern California, lies 30 mi SSW of Santa Barbara. It is the 2nd largest of these islands at 55,000 a. Geologically, Santa Rosa is made up of a complexly faulted sequence of Eocene through Miocene sandstone,

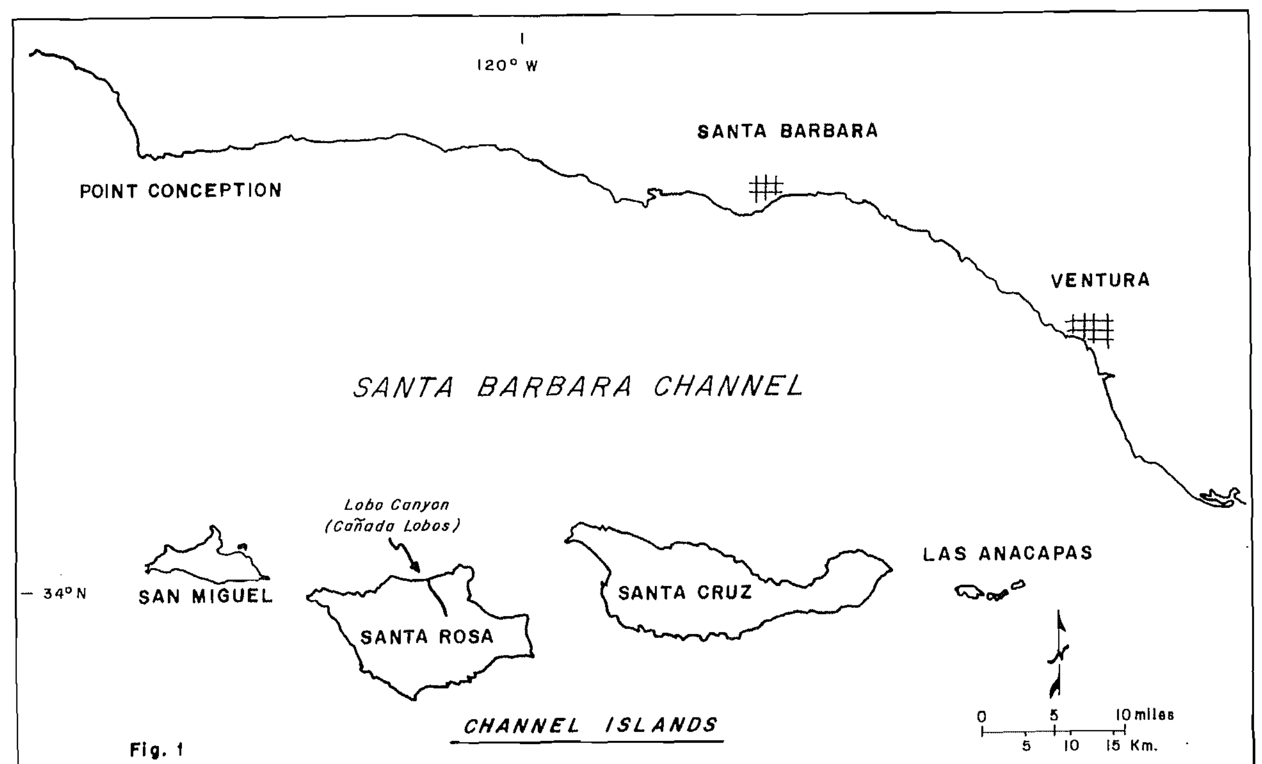

Figure 1. Location of Santa Rosa Island.